



Gamma radiation effect on the chemical, mechanical and thermal properties of PCL/MCM-48-PVA nanocomposite films

Marcos Vinícius da Silva Paula^a, Leandro Araújo de Azevedo^b,
Ivo Diego de Lima Silva^c, Carlos Alberto Brito da Silva Jr.^{d,*}, Glória Maria Vinhas^c,
Severino Alves Jr.^b

^a Faculdade de Engenharia de Materiais, Universidade Federal Do Pará, Ananindeua, 67113-901, Brazil

^b Laboratório de Terras Raras, Universidade Federal de Pernambuco, Pernambuco 50670-901, Brazil

^c Departamento de Engenharia Química, Universidade Federal de Pernambuco, Pernambuco 50670-901, Brazil

^d Faculdade de Física, Universidade Federal Do Pará, Ananindeua, 67113-901, Brazil

ARTICLE INFO

Keywords:

Polycaprolactone (PCL)
poly(vinyl alcohol) (PVA)
Nanocomposite (NC) films
Gamma radiation
MCM-48-M
Chemical properties

ABSTRACT

In this work, poly (vinyl alcohol) (PVA) was employed to produce a Mesoporous Composition of Matter-48 Modified (MCM-48-M or MCM-48-PVA). After surface modification, MCM-48-M was used to produce nanocomposite (NC) films with polycaprolactone (PCL) as a matrix at room temperature. PCL and MCM-48 nanoparticles (NPs) were chosen due to their great biocompatibility and low toxicity. However, MCM-48-M is more compatible with PCL than MCM-48. NC films were sterilized by gamma radiation with a dose of 25 kGy and characterized by experimental techniques to investigate their chemical, mechanical (tensile) and thermal properties. Scanning electron microscopy (SEM) and transmission electronic microscopy (TEM) results indicated that MCM-48-M exhibited a random distribution in the PCL matrix. The PCL chemical structure was preserved in NC films as described by Fourier transform infrared (FT-IR) spectroscopy as well as the tensile and thermal properties of NC films. FT-IR and thermogravimetric analysis (TGA) results showed surface modification. X-ray diffraction (XRD) and differential scanning calorimetry (DSC) showed that crystalline symmetries were preserved and the crystallinity of NC films had small variations in all samples before and after irradiation, respectively. But, our results did not indicate major changes showing that this method is successful for the sterilization of PCL/MCM-48-PVA NC films.

1. Introduction

Polycaprolactone (PCL) is a thermoplastic polyester, which is hydrophobic and semi-crystalline, with a melting temperature around 60 °C. It is biocompatible, biodegradable formed by hexanoate repeating units and exhibits excellent flexibility [1–5]. PCL is used in tissue regeneration [6], controlled drug delivery [7], implants and food packaging [8], wound dressing [9], among other applications. PCL may not have satisfactory properties for certain applications, such as hydrophilicity for tissue engineering applications, tensile properties in implants, and osteoconductivity [10–12]. PCL properties can be refined through the addition of nanomaterials to the polymer, resulting in polymer matrix nanocomposites (PMNCs) [13,14].

* Corresponding author.

E-mail address: cabsjr@ufpa.br (C.A. Brito da Silva).

<https://doi.org/10.1016/j.heliyon.2023.e18091>

Received 28 February 2023; Received in revised form 5 July 2023; Accepted 6 July 2023

Available online 7 July 2023

2405-8440/© 2023 Published by Elsevier Ltd.

This is an open access article under the CC BY-NC-ND license

(<http://creativecommons.org/licenses/by-nc-nd/4.0/>).

PMNCs are obtained through various methods such as extrusion [15], 3D printing [16], solvent casting [17], and polymerization [18], among others. Solvent casting is a simple, inexpensive method that does not require sophisticated equipment and is widely used to produce PMNCs [19]. Wang et al. using thermal extrusion technology characterized PCL filaments with hydroxyapatite (HA) as a 3D printing material to obtain scaffolds for bone tissue engineering. These scaffolds exhibited good hydrophilicity and better tensile properties compared to PCL scaffolds [20]. Augustine et al. obtained better tensile properties, antimicrobial properties, and fibroblast proliferation for PCL membranes with ZnO nanoparticles (ZnONPs) via electrospinning [21]. Díez-Rodríguez et al. prepared NCs based on PCL by melt extrusion with SBA-15 mesoporous silica that exhibited satisfactory tensile properties compared to PCL [22]. Elen et al., using a melt-blending technique, prepared NCs of PCL with different morphologies of ZnO for use in food packaging. Electron microscopy images revealed a good dispersion of ZnO nanoparticles in the polymer matrix causing a decrease in the permeability of gases, which was ascribed to the adsorption of gases and the production of a tortuous route [23]. PVA membranes with Ag nanoparticles (AgNPs) were obtained by electrospinning and modified with 3,3',4,4'-benzophenone tetracarboxylic acid (BPTA). The PVA/AgNPs/BPTA membrane exhibited higher antibacterial activity compared to other membranes investigated [24].

Mobil Composition of Matter No. 48 (MCM-48) is the name given for a series of mesoporous materials that were first synthesized by researchers at Mobil Oil Corporation in 1992. MCM-48 is one of the most popular mesoporous molecular sieves that are intensively studied. It is a nanomaterial used in NCs to refine the properties of a given polymer [25]. MCM-48 is a member of the M41S family, which exhibits an ordered porous structure of SiO₂ and includes silanol groups (Si–OH) [26,27]. MCM-48 is a nanomaterial with a cubic structure that belongs to the *Ia3d* space group exhibiting thermal stability, and biocompatibility, which can be used in thermal stabilization of polymers and in biomedical applications [25,26,28]. Nanometer-scale materials such as MCM-48, however, may not have sufficient dispersion within a polymeric matrix due to their high surface energy, which may compromise the properties of NCs [29]. This dispersion of MCM-48 in a polymeric matrix such as PCL can be maximized by modifying the MCM-48 surface with reagents that provide a large distance between the NPs and a greater chemical affinity with the polymeric matrix, improving its dispersion in the polymer [30]. Among these reagents, PVA can be used to perform surface modification of MCM-48 for better dispersion in PCL.

PVA is a hydrophilic semi-crystalline polymer that has biocompatibility, good film-forming ability, and an ability to interact with inorganic or organic materials [31,32]. Mallakpour and Khani modified the surface of amorphous SiO₂NPs with thiamine. After this modification, they obtained PCL-modified SiO₂NCs which exhibited bioactivity [33]. Similarly, Mallakpour and Nouruzi modified ZnONPs with PVA to obtain NC films with PCL, observing that the modified ZnONPs with PVA showed desirable dispersion in the PCL matrix [34]. Paula et al. carried out surface modification of MCM-48 with (3-Aminopropyl)triethoxysilane (APTES) into the PCL matrix to obtain NC films, achieving positive distribution in the PCL matrix [35]. Lopez-Figuera et al. prepared PCL/MCM-41 composites functionalized with *N*-[3-(trimethoxysilyl)propyl]-ethylenediamine (EPTES) via in situ polymerization that exhibited better thermal properties, ascribed to the interaction between PCL and the MCM-41-EPTES [11]. Mallakpour and Nouruzi performed the surface modification of ZnONPs with citric acid via ultrasound and then added the modified NPs to PCL matrix to obtain NC films. They observed that the tensile strength, increased from 13.01 MPa for PCL film to 22.23 MPa for NC film with 2% modified ZnO [36].

PCL NCs are used in biomaterials and food packaging [35,37], but require the sterilization of materials to eliminate microorganisms through exposure to gamma radiation at 25 kGy - considered the gold standard to eliminate microorganisms [38]. Exposure of PCL NCs to gamma radiation can compromise their tensile properties and chemical characteristics [39]. The gamma radiation can cause the scissions of polymeric chains and/or the formation of crosslinking between the polymeric chains, which can decrease or increase in tensile properties, respectively [40]. The scission of chains or the formation of crosslinking between the chains depends on factors such as dose, dose rate, irradiation conditions, and polymer chemistry [41].

Investigations have been carried out on the influence of ionizing radiation on the PCL. Cottam et al. observed the chain scission and the formation of crosslinking in PCL scaffolds exposed at 25 kGy [42]. Masson et al., after exposing nanospheres of PCL at 25 kGy, found only the creation of crosslinking between polymer chains [43]. Cooke et al., after irradiating PCL scaffolds with X-ray photons, immersed in an aqueous environment, in therapeutic doses up to 50 Gy, found the formation of crosslinking between the polymer chains, with a consequent decrease of 8% in the degree of crystallinity of the PCL [41]. These results agree with Pereira-Loch et al. that improved the tensile properties of polymeric immobilization devices of PCL using radiotherapy irradiated in a linear accelerator up to 420 Gy to form crosslinking between the chains of the polymer [44]. Bosworth et al. exposed electrospun PCL fibers to gamma radiation at 0, 15, 20, 25, 30, 35, 40, and 45 kGy to observe the chain scission effect proportional to applied dose, i. e., increasing the applied dose decreased the molecular weight average molar mass. They also reported, that through infrared spectroscopy results, the presence of new vibrational modes was not observed in samples irradiated up to 45 kGy [45].

Thus, the main goal of this paper was to carry out the superficial modification of MCM-48 with PVA (MCM-48-PVA or MCM-48-M) to evaluate the influence of gamma radiation at 25 kGy on the chemical, tensile and thermal properties of NC films (PCL/MCM-48-PVA). The films were produced via solvent casting with MCM-48-M content equal to 0.5% in relation to PCL and irradiated at 25 kGy at room temperature.

2. Materials and methods

2.1. Materials

Cetyltrimethylammonium bromide (CTAB) (98%), Pluronic® F-127), Tetraethyl orthosilicate (TEOS) (98%), and ammonium hydroxide were supplied by Sigma Aldrich. Ethanol and chloroform were acquired from Dinâmica. High molecular weight PVA was supplied by Alfa Aesar (degree of hydrolysis: 98–99% and the degree of polymerization is given by relation molar/repeating unit mass: 88,000 g/mol-97,000 g/mol). PCL was obtained from Capa™ (PCL 6500). All reagents were analytical grade and used without prior

treatment.

2.2. Synthesis of MCM-48

The MCM-48 was synthesized according to the previous methodology with modifications [28]. First, 0.5 g of CTAB and 2.05 g of F127 were added to 96 mL of distilled water. After, 43 mL of ethanol was added to 10.05 g of a 29% ammonium hydroxide solution. The mixture remained under agitation until achieving homogeneity with the subsequent addition of 1.8 g of TEOS. The suspension remained under agitation for 10 min with the subsequent storage for 12 h at room temperature. After that, the mixture was centrifuged for 30 min at 6000 rpm. A white solid was rinsed with distilled water and submitted to centrifugation process at 6000 rpm and 30 min then the solid remained for 12 h at 70 °C to which it was placed in a Teflon reactor with 8.5 mL of distilled water at 140 °C for 48 h. Subsequently, the solid remained for 4 h at 550 °C.

2.3. Modification of MCM-48 with PVA

The modification of MCM-48 with PVA was performed based on the literature methodology, with some modifications [34]. First, 100 mg of MCM-48 was placed in 10 ml of distilled water with subsequent exposure to an ultrasonic bath for 30 min. After, 100 mg of PVA was added to 10 mL of distilled water and added to the previously obtained mixture. The mixture was stirred for 2 h and sonicated at 30 min in an ultrasonic bath. After that, the mixture was centrifuged at 6000 rpm for 30 min and the solid remained at room temperature for 24 h.

2.4. Preparation of nanocomposite films

PCL and NC films with a content of 0.5% of modified silica were obtained by solvent casting as illustrated in Fig. 1. The films obtained in this investigation are described in Table 1. Pre-calculated amounts of MCM-48 and MCM-48-M were added to 5 mL of chloroform and placed in an ultrasonic bath for 30 min. After, MCM-48 or MCM-48-M dispersed in 5 mL of chloroform was added to 2.5 g of PCL and 50 mL of chloroform. The mixture remained in stirring for 48 h. After this period, the mixture was added to a glass plate and the chloroform was eliminated under slow evaporation for 48 h at room temperature. The films were placed in a desiccator using silica and stored for further characterization [46].

2.5. Irradiation of films

The samples were irradiated from a source of $^{60}\text{Cobalt}$ (Gammacell GC220 Excel irradiator - MDS Nordion, Canada) at 25 kGy (rate of 2.157 kGy/h, for a period of time equal to 11:35 h), with air at room temperature.

2.6. Fourier transform infrared spectroscopy (FT-IR)

Absorption spectra in the infrared (IR) region by attenuated total reflectance were acquired at room temperature in a PerkinElmer FT-IR/FT-NIR spectrophotometer Spectrum 400 Bruker. Spectra were obtained with a resolution of 4 cm^{-1} , 32 scans, and a selection of waves situated between 4000 cm^{-1} to 522.5 cm^{-1} .



Fig. 1. Schematic diagram of PCL/MCM-48-M film preparation, where M = PVA.

Table 1
Description of film composition.

Sample	Composition
F0	Polycaprolactone
F1	Polycaprolactone + MCM-48
F2	Polycaprolactone + MCM-48-PVA
F3	Polycaprolactone irradiated at 25 kGy
F4	Polycaprolactone + MCM-48 irradiated at 25 kGy
F5	Polycaprolactone + MCM-48-PVA irradiated at 25 kGy

2.7. Thermogravimetric analysis (TGA)

TGA curves for the samples were acquired with SHIMADZU DTG-60H instrument, under an inert nitrogen atmosphere (100 mL/min) in a range from room temperature to 600 °C at a rate of 10 °C/min.

2.8. X-ray diffraction (XRD)

The diffractograms of the films were determined in a Bruker D8 Advance X-ray diffractometer with Cu K α ($\lambda = 0.15$ nm), with a scanning speed of 0.02° min⁻¹.

2.9. Differential scanning calorimetry (DSC)

DSC curves were acquired in a differential scanning calorimeter, model 1 Star* system (Mettler Toledo). DSC curves were performed under an inert nitrogen atmosphere with the conditions: 1) 0 °C–80 °C, at a rate of 10 °C/min; 2) cooling to 0 °C, at a rate of 20 °C/min; and 3) 0 °C–80 °C, at a rate of 10 °C/min [23]. The degree of crystallinity X_c was calculated using the equation below, ΔH_m equals melting enthalpy of the polymer in the composite, %pol equals content of polymer in the NC and ΔH_{ref} equals 100% crystalline melting enthalpy of the polymer. The value employed for ΔH_{ref} was 139.3 J/g [47].

$$X_c = \Delta H_m / (\%pol \cdot \Delta H_{ref})$$

2.10. Scanning electron microscopy (SEM)

SEM images were acquired by a microscope (Tescan Mira3), with an accelerating voltage of 10 kV.

2.11. Transmission electronic microscopy (TEM)

NC film images were determined via transmission electron microscope – TEM (Jeol, model JEM-2100), with an accelerating voltage of 200 kV. Drops of the samples in dichloromethane were placed on copper grids.

2.12. Tensile properties

Tensile Properties of films were performed on an Instron machine EMIC, DL-500 N, crosshead speed of 5 mm/min. Average results were calculated for two samples of each film. Duncan's test was performed to determine significant statistical variations.

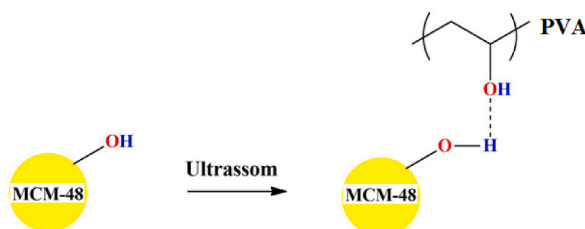


Fig. 2. Surface modification of MCM-48 with PVA.

3. Results and discussion

3.1. Fourier transform infrared spectroscopy (FT-IR)

The surface of the MCM-48 was modified with PVA. As seen in Fig. 2, interactions between MCM-48 and PVA were performed by hydrogen bonds between the silanol groups on the surface of MCM-48 and the OH groups of the PVA chains. F2 films were obtained via solvent casting. The influence of gamma radiation at 25 kGy on the chemical, tensile and thermal properties of F2 (MCM-48-PVA) films will be described in the following sections.

FT-IR spectra were obtained to determine the effects of gamma radiation at 25 kGy for NC films. Fig. 3 shows the acquired spectra for MCM-48, MCM-48-M, and PVA. In the MCM-48 spectrum, a vibrational mode is visualized at 3400 cm^{-1} referring to Si–OH stretching. The vibrational modes observed at 800 cm^{-1} and 1051 cm^{-1} are attributed to the symmetrical and asymmetric stretching for Si–O–Si [48], respectively. For the MCM-48-M, almost the same spectral behavior was observed in comparison to the MCM-48 spectrum. Nevertheless, the presence of surface modification with PVA can be observed through the TGA results (see section 3.2). Small shifts in the absorption bands for MCM-48-M compared to MCM-48 were attributed to hydrogen bonding between the O–H group of PVA and the silanol group of MCM-48 (Fig. 4) [34]. The PVA exhibited a band centered at 3280 cm^{-1} , originated from the OH bonds of the polymer and water molecules adsorbed on its surface [49]. The bands at 2942 cm^{-1} and 1088 cm^{-1} are attributed to stretches of the C–H and C–O groups, respectively [50]. The band at 1713 cm^{-1} occurs due to the presence of the carbonyl group, resulting from obtaining PVA from the hydrolysis of poly (vinyl acetate) [51].

Fig. 4 shows the spectra for F2 and F5 films. The polymer exhibited a band at 1722 cm^{-1} , attributed to the C=O stretching of the PCL, the bands observed at 2948 cm^{-1} and 2868 cm^{-1} occur due to symmetric and asymmetric stretching of C–H bonds in the PCL [33, 34]. F1 and F2 films exhibited a spectral behavior similar to observed for PCL, where the bands assigned to C–H bonds and carbonyl were observed around 2950 cm^{-1} , 2870 cm^{-1} , and 1722 cm^{-1} , respectively. Spectral similarity with PCL was also observed for F4 and F5 films irradiated at 25 kGy, with the presence of the characteristic bands of the polymer attributed as C–H and carbonyl bonds around 2950 cm^{-1} , 2870 cm^{-1} , and 1722 cm^{-1} , respectively. These results indicate that the chemical structure of the polymer is preserved after irradiation at 25 kGy. These findings agree with the results reported by Subramanian et al., where sterilized PCL nanofibers containing *Gymnema sylvestri* leaf extract via gamma radiation. They observed that irradiation at 25 kGy did not alter the chemical structure of the nanofibers [52]. Similarly, Augustine et al. based on FT-IR results, revealed that the chemical composition of PCL in electrospun membranes is preserved after irradiation at 25 kGy [21]. Our FT-IR results demonstrated that the irradiation at 25 kGy did not change the chemical identity of the polymer in the evaluated NC films.

3.2. Thermogravimetric analysis (TGA)

The thermal stability of the samples was performed by thermogravimetric analysis (TGA). Fig. 5 shows the TGA curves for MCM-48-M and PVA. The MCM-48-M had a mass loss event close to $100\text{ }^{\circ}\text{C}$, ascribed as the removal of water physically bound to the surface of MCM-48-M. It also showed mass loss events between $200\text{ }^{\circ}\text{C}$ and $600\text{ }^{\circ}\text{C}$, which are described as the elimination of organic content, which corroborates that the surface of MCM-48 was modified with PVA. These results are in agreement with our previous study: where the surface of MCM-48 was modified with APTES, it was observed that modified MCM-48 had a first event close to $100\text{ }^{\circ}\text{C}$ attributed to the elimination of water; and a second event which was assigned to the surface modification with APTES [35]. Pure PVA had a first mass loss between $60\text{ }^{\circ}\text{C}$ and $200\text{ }^{\circ}\text{C}$ originating from the loss of adsorbed water [53]. A second event was also observed for PVA

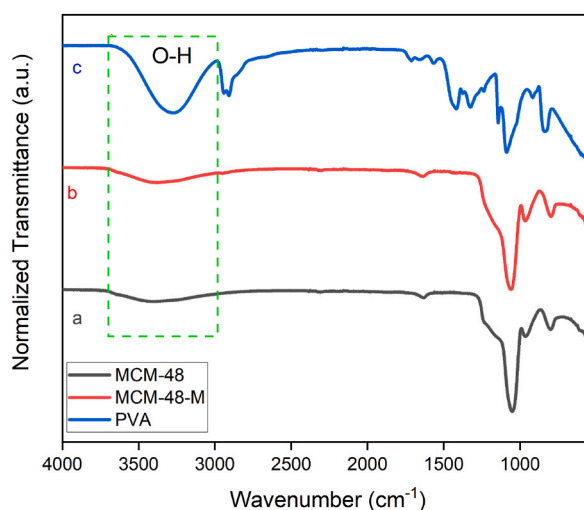


Fig. 3. FT-IR spectra of (a) MCM-48; (b) MCM-48-M; (c) PVA.

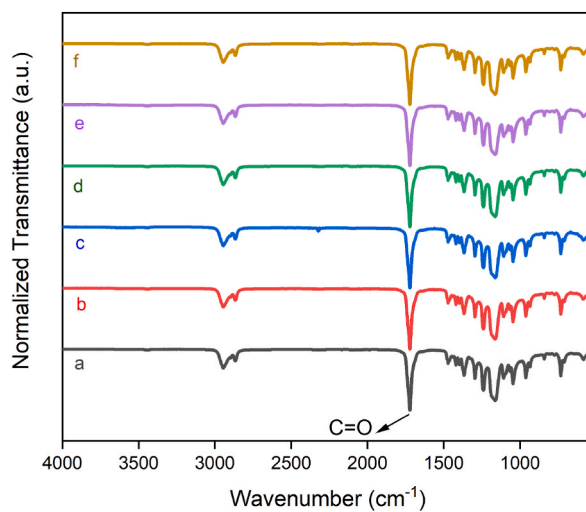


Fig. 4. FT-IR spectra of (a) F0; (b) F1; (c) F2; (d) F3; (e) F4; (f) F5.

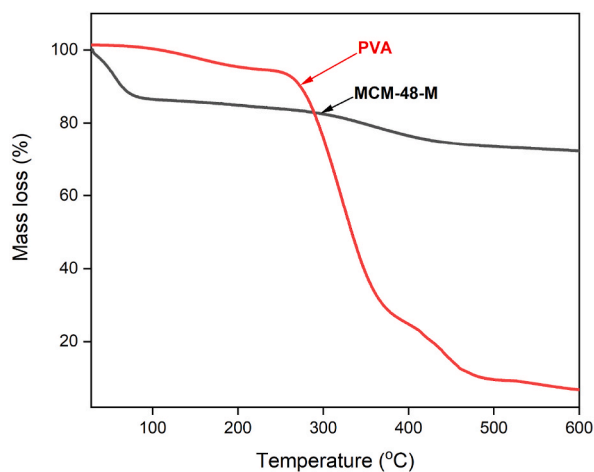


Fig. 5. TGA curves of MCM-48-M and PVA.

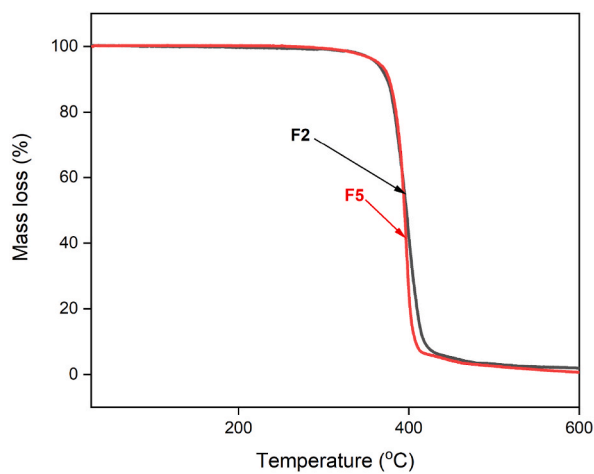


Fig. 6. TGA curves of F2 and F5.

between 210 °C and 350 °C, arising from water elimination reactions [54]. The last event between 390 °C and 550 °C was associated with the thermal decomposition of polyenes, producing carbon and hydrocarbons [55].

Fig. 6 shows the TG curves for F2 and F5 films. The samples exhibited a single mass loss event between 200 and 500 °C, this event was associated with the decomposition of the PCL [56,57]. This thermal behavior was similar to that observed for PCL in our previous study, revealing that the thermal stability of the polymer is preserved after the insertion of MCM-48-M and irradiated at 25 kGy [35]. The absence of mass loss events characteristic of the thermal decomposition of MCM-48 such as loss of water adsorbed was attributed to the low content of MCM-48 in the PCL matrix, however the presence of MCM-48-M in NC films was confirmed by SEM and TEM images (Sections 3.5 and 3.6). Table 2 presents the temperatures referring to the mass loss of 5% (T_5), 10% (T_{10}), 50% (T_{50}), T_{max} (maximum temperature of degradation), and also char yield at 600 °C. Table 2 shows that the T_5 , T_{10} , T_{50} , and T_{max} values for F2 and F5 were similar before and after exposure at 25 kGy. These results are similar to those shown in our previous study for T_5 , T_{10} , and T_{50} for PCL/MCM-48 films irradiated at 25 kGy [35]. TGA data demonstrated that the thermal decomposition characteristics of F2 practically did not differ from the thermal decomposition characteristics exhibited by F5.

3.3. X-ray diffraction (XRD)

The crystalline profile of F2 and F5 films was accessed by X-ray diffraction. Fig. 7 shows the diffractograms for F2 and F5 films. For the F2 film, three angles of reflection were observed, at 21.3°, 21.9°, and 23.6°, which are described to the planes (110), (111), and (200) of the PCL orthorhombic unit cell [21,28,36,58]. The F2 and F5 films, exhibited the same semi-crystalline behavior, characteristic of PCL. The presence of characteristic angles of MCM-48 in the F2 and F5 films was not observed, this absence can be due to the low content of MCM-48-M in the NC films [36,58]. Mallakpour and Nouruzi found similar results for PCL films with diacid-modified ZnO nanoparticles [59]. The F2 and F5 films demonstrated no changes in the semi-crystalline profile of the PCL, which confirms that the irradiation at 25 kGy did not modify the semi-crystalline behavior of the polymeric matrix.

3.4. Differential scanning calorimetry (DSC)

DSC curves were obtained in an inert atmosphere to quantify the degree of crystallinity of samples F2 and F5. DSC curves for F2 and F5 are displayed in Fig. S1 (Supplementary Material). Table 3 shows T_c (crystallization temperature), T_m (melting temperature), ΔH_m (melt enthalpy), and X_c (degree of crystallinity) for the samples analyzed. Recently we observed that the PCL had a T_m equal to 61.3 °C [35]. In this investigation, it is observed that the addition of MCM-48-M to the PCL matrix did not produce a significant change in T_m in relation to pure PCL, the same behavior was observed for sample F5. The degree of crystallinity showed no greater change for sample F5 compared to F2. This same result profile was observed for T_c and ΔH_m for the films of samples F2 and F5. In our previous study, we also observed that the addition of MCM-48 modified with APTES did not produce significant changes in DCS results for NC films after irradiation at 25 kGy [35]. Elen et al. reported that the presence of ZnO nanoparticles in the PCL matrix did not produce significant variations in the values of T_c , T_m , ΔH_m , and X_c [23]. Li et al., prepared chitin nanofibril/polycaprolactone NC fiber mats by electrospinning. They also observed that the addition of a low concentration of chitin, such as 5%, did not cause greater changes in the DSC results compared to pure PCL [60]. Our results showed that the exposure of F2 films at 25 kGy caused marginal variations in T_c , T_m , ΔH_m , and X_c .

3.5. Scanning electron microscopy

The surface morphology of the materials was evaluated through the acquisition of SEM images. Fig. 8 displays SEM images for the MCM-48 and MCM-48-M. For the MCM-48, a spherical shape is observed; this morphology is also observed for the MCM-48-M. These findings confirm that the morphology of MCM-48 is preserved after surface modification with PVA. Similar results were reported for MCM-48 functionalized with APTES [61,62].

Fig. 9 shows the SEM images for the surface and lateral surface of F1 and F2 films. The MCM-48 and MCM-48-M are randomly distributed in the PCL matrix. The random distribution of MCM-48 and MCM-48-M in the PCL matrix was attributed to the interactions formed between the fillers and the polymer and nanometric dimensions of the fillers. Similar results to ours were observed by Mallakpour and Khani [33]. Lopes-Figueroas and collaborators observed a good distribution of MCM-41 modified with EPTES in composite films with PCL [11].

3.6. Transmission electronic microscopy

Fig. 10 shows the TEM images for F1 and F2 films. Fig. 10a and b confirmed that MCM-48 and MCM-48-M have a spherical morphology and nanometric dimensions and are randomly dispersed in the PCL matrix. Fig. 10a and b also shows the histograms for

Table 2
Thermal properties of F2 and F5.

Sample	T_5 (°C)	T_{10} (°C)	T_{50} (°C)	T_{max} (°C)	Char yield at 600 °C (%)
F2	362	374	397	401	1.98
F5	364	377	395	400	0.67

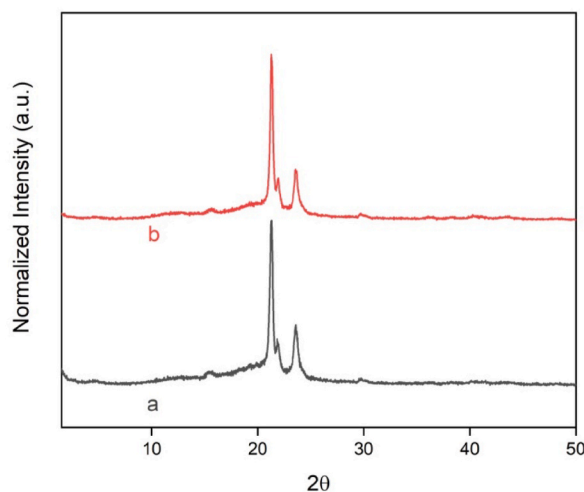


Fig. 7. XRD curves of (a) F2 and (b) F5.

Table 3

Melting point temperature, crystallization temperature, enthalpy of melting, and degree of crystallinity for F2 and F5.

Sample	T_c (°C)	T_m (°C)	ΔH_m (J/g)	X_c (%)
F2	24.21	64.96	52.32	37.56
F5	25.60	61.20	55.32	39.72

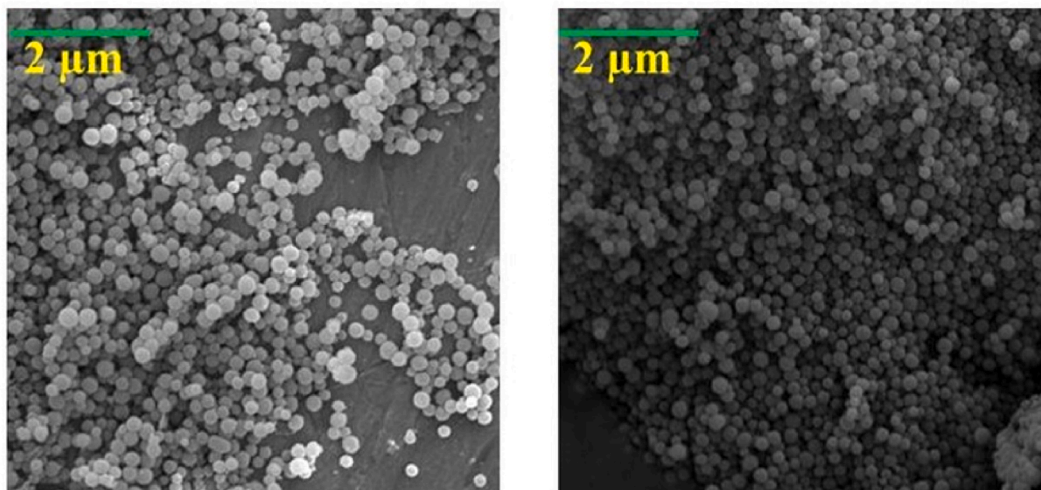


Fig. 8. SEM images of MCM-48 (left) and MCM-48-M (right).

the size distribution for MCM-48 and MCM-48-M in NC films. The average particle sizes calculated for MCM-48 and MCM-48-M in the PCL matrix were 170.1 nm and 203.9 nm, respectively. The increase in average particle size for MCM-48-M, in the F2 film, can be described as a result of surface modification with PVA. Kim et al. also observed an increase in the size of silica nanoparticles after surface modification with poly (methyl methacrylate) [63].

3.7. Tensile properties

The results of the tensile properties of the F2 and F5 films are described in Table 4. Table 4 presents the mean values for the tensile strength (σ), modulus of elasticity (ϵ), and elongation at break (E_b). Duncan's test was employed to evaluate mean values with a significance level of 5%. Our results revealed that through Duncan's test, no statistically significant difference was found for σ , ϵ , and E_b for F2 and F5 films. However, E_b exhibited a high variation this can be attributed to surface modification of the nanoparticles. After

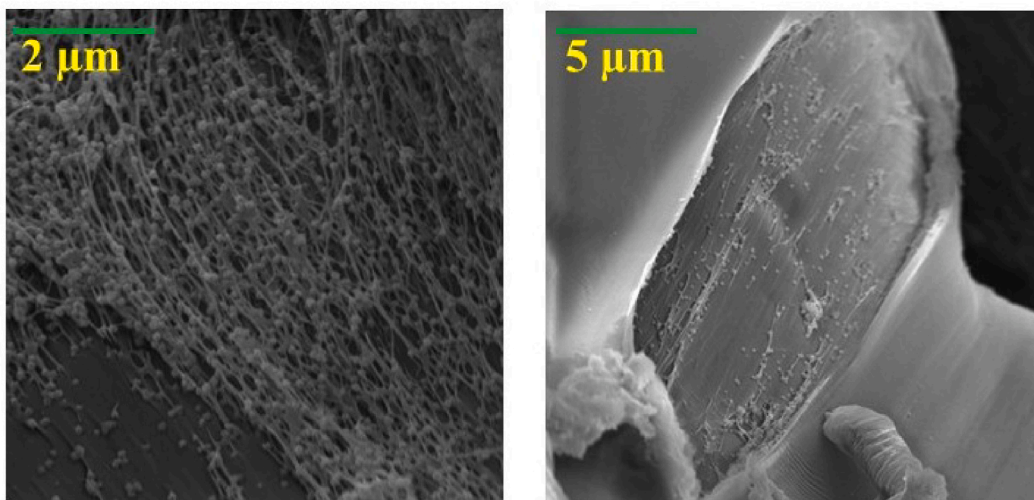


Fig. 9. SEM images of lateral surface of F1 (left) and (b) lateral surface of F2 (right).

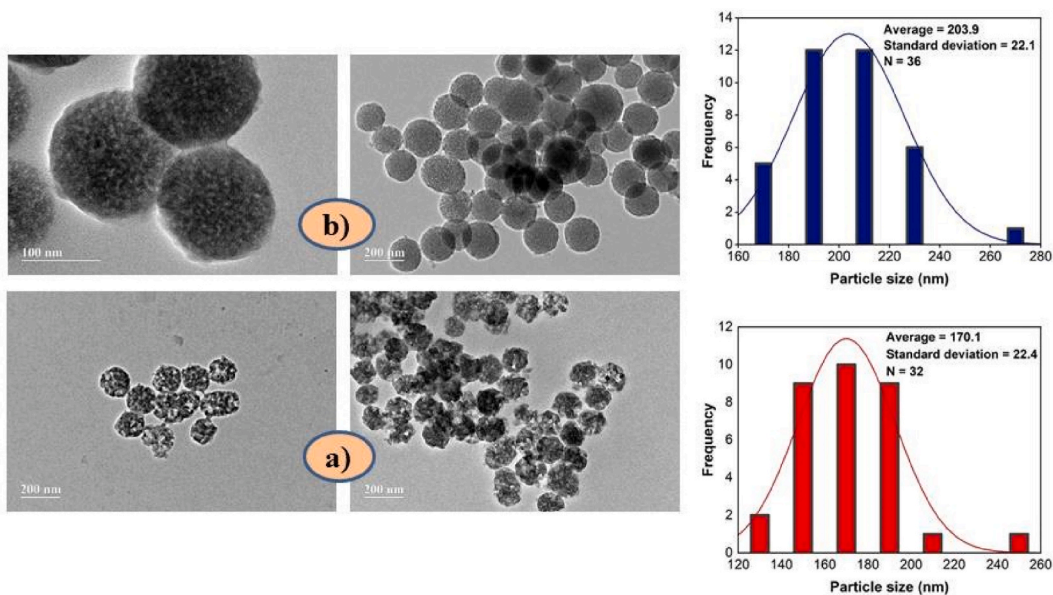


Fig. 10. TEM images of (a) F1; (b) F2.

Table 4
Tensile properties for F2 and F5.

Sample	σ (MPa)	ϵ (MPa)	Eb (%)
F2	8.17 ± 2.29^a	152.25 ± 15.13^a	57.99 ± 31.45^a
F5	9.70 ± 0.12^a	153.50 ± 5.58^a	72.48 ± 19.66^a

modification the nanoparticles increased their average particle sizes (as observed by the TEM images) which can form stress points, increasing the variation in measurements for Eb. Similar results were reported for σ and ϵ in our previous studies [35]. Tension property findings showed that there was no statistically significant difference between the films of samples F2 and F5.

Means followed by the same letters in each column do not differ significantly ($p < 0.05$) by the Duncan test.

4. Conclusions

The surface of the MCM-48 was modified with PVA with the support of an ultrasonic bath as described by our FT-IR and TGA results. SEM and TEM images showed that MCM-48-M has a spherical morphology and nanometric dimensions. F2 films were produced by the solvent casting method. MCM-48-M was randomly distributed in the PCL matrix as seen in the SEM and TEM images. FT-IR results indicated that the PCL structure was preserved after exposure at 25 kGy. The XRD results confirm the semi-crystalline profile of the polymer is preserved after irradiation at 25 kGy. The tensile and thermal properties of F2 and F5 films had marginal variations. Our findings indicated that irradiation at 25 kGy was not able to promote significant changes in the chemical, thermal, and tensile properties of F2 films.

Author contribution statement

M.V.S. Paula, L.A. Azavedo, and I.D. Lima: Conceived and designed the experiments; Performed the experiments.
G.M. Vinhas and S. Alves Jr: Analyzed and interpreted the data; Contributed reagents, materials, analysis tools or data.
C.A.B. Silva Jr.: Analyzed and interpreted the data; Wrote the paper.

Funding statement

C.A.B. Silva Jr. thanks PROPESP/UFPA-PIBIC Interior (PRO5142-2021).

Data availability statement

Data included in article/supplementary material/referenced in article.

Declaration of competing interest

The authors declare that they have no known competing financial interests or personal relationships that could have appeared to influence the work reported in this paper.

Appendix A. Supplementary data

Supplementary data to this article can be found online at <https://doi.org/10.1016/j.heliyon.2023.e18091>.

References

- [1] M. Labet, W. Thielemans, Synthesis of polycaprolactone: a review, *Chem. Soc. Rev.* 38 (2009) 3484–3504, <https://doi.org/10.1039/B820162P>.
- [2] M.A. Woodruff, D.W. Hutmacher, The return of a forgotten polymer—polycaprolactone in the 21st century, *Prog. Polym. Sci.* 35 (2010) 1217–1256, <https://doi.org/10.1016/j.progpolymsci.2010.04.002>.
- [3] M.E. El-Naggar, A.M. Abdelgawad, R. Abdel-Sattar, A.A. Gibriel, B.A. Hemdan, Potential antimicrobial and antibiofilm efficacy of pepper mint Oil nanoemulsion loaded polycaprolactone nanofibrous scaffolds, *Eur. Polym. J.* 184 (2023), 111782, <https://doi.org/10.1016/j.eurpolymj.2022.111782>.
- [4] Z. Cai, C. Shen, Z. Deng, D. Wu, K. Chen, Solution blow spinning of multilayer polycaprolactone/curcumin-loaded gelatin/polycaprolactone nanofilm for slow release and bacterial inhibition, *Food Hydrocol. Health* 2 (2022), 100062, <https://doi.org/10.1016/j.fhfh.2022.100062>.
- [5] L. Aliotta, V. Gigante, R. Geerink, M.B. Coltelli, A. Lazzeri, Micromechanical analysis and fracture mechanics of Poly(lactic acid) (PLA)/Polycaprolactone (PCL) binary blends, *Polym. Test.* 121 (2023), 107984, <https://doi.org/10.1016/j.polymertesting.2023.107984>.
- [6] K. Liu, et al., Effect of polycaprolactone impregnation on the properties of calcium silicate scaffolds fabricated by 3D printing, *Mater. Des.* 220 (2022), 110856, <https://doi.org/10.1016/j.matdes.2022.110856>.
- [7] M. Furko, et al., Biomimetic mineralized amorphous carbonated calcium phosphate-polycaprolactone bioadhesive composites as potential coatings on implant materials, *Ceram. Int.* 49 (2023) 18565–18576, <https://doi.org/10.1016/j.ceramint.2023.02.231>.
- [8] Z. Cai, C. Shen, Z. Deng, D. Wu, K. Chen, Solution blow spinning of multilayer polycaprolactone/curcumin-loaded gelatin/polycaprolactone nanofilm for slow release and bacterial inhibition, *Food Hydrocol. Health* 2 (2022), 100062, <https://doi.org/10.1016/j.fhfh.2022.100062>.
- [9] X. Liu, et al., Polycaprolactone nanofiber-alginate hydrogel interpenetrated skin substitute for regulation of wound-substitute interface, *Mater. Des.* 227 (2023), 111706, <https://doi.org/10.1016/j.matdes.2023.111706>.
- [10] H. Jahani, et al., Controlled surface morphology and hydrophilicity of polycaprolactone toward selective differentiation of mesenchymal stem cells to neural like cells, *J. Biomed. Mater. Res.* 103 (2015) 1875–1881, <https://doi.org/10.1002/jbm.a.35328>.
- [11] L. Lopez-Figueras, N. Navascues, S. Irusta, Polycaprolactone/mesoporous silica MCM-41 composites prepared by in situ polymerization, *Particuology* 30 (2017) 135–143, <https://doi.org/10.1016/j.partic.2016.05.005>.
- [12] J.M. Fernandez, M.S. Molinuevo, M.S. Cortizo, A.M. Cortizo, Development of an osteoconductive PCL-PDIPF-hydroxyapatite composite scaffold for bone tissue engineering, *J. Tissue Eng. Regen. Med.* 5 (2011) e126–e135, <https://doi.org/10.1002/term.394>.
- [13] S.P. Davtyan, A. Berlin, V. Agabekov, N. Lekishvili, Synthesis, properties, and applications of polymeric nanocomposites, *J. Nanomater.* 2012 (2012), 215094, <https://doi.org/10.1155/2012/215094>.
- [14] P.H.C. Camargo, K.G. Satyanarayana, F. Wypych, Nanocomposites: synthesis, structure, properties and new application opportunities, *Mater. Res.* 12 (2009) 1–39, <https://doi.org/10.1590/S1516-14392009000100002>.
- [15] J. Sanes, C. Sánchez, R. Pamies, M.D. Avilés, M.D. Bermúdez, Extrusion of polymer nanocomposites with graphene and graphene derivative nanofillers: an overview of recent developments, *Mater* 13 (2020) 549, <https://doi.org/10.3390/ma13030549>.
- [16] W.H.Y. Clarissa, C. H Chia, S. Zakaria, Y.C.Y. Evyan, Recent advancement in 3-D printing: nanocomposites with added functionality, *Prog. Addit. Manuf.* 7 (2022) 325–350, <https://doi.org/10.1007/S40964-021-00232-z/figures/8>.

- [17] K. Ghosal, et al., Antibacterial photodynamic activity of hydrophobic carbon quantum dots and polycaprolactone based nanocomposite processed via both electrospinning and solvent casting method, *Photodiagnosis Photodyn. Ther.* 35 (2021), 102455, <https://doi.org/10.1016/j.pdpdt.2021.102455>.
- [18] H. Althues, P. Simon, S. Kaskel, Transparent and luminescent YVO₄ : Eu/polymer nanocomposites prepared by in situ polymerization, *J. Mater. Chem.* 17 (2007) 758–765, <https://doi.org/10.1039/b611917d>.
- [19] L. Pazourková, G.S. Martynková, D. Plachá, Preparation and mechanical properties of polymeric nanocomposites with hydroxyapatite and hydroxyapatite/clay mineral fillers – review, *J. Nanotechnol. Nanomed. Nanobiotechnol.* 2 (2015) 1–8, <https://doi.org/10.24966/ntmb-2044/100007>.
- [20] F. Wang, et al., Fabrication and characterization of PCL/HA filament as a 3D printing material using thermal extrusion technology for bone tissue engineering, *Polymers* 14 (2022) 669, <https://doi.org/10.3390/polym14040669/s1>.
- [21] R. Augustine, H.N. Malik, D. Kumar, A. Mukherjee, Electrospun polycaprolactone/ZnO nanocomposite membranes as biomaterials with antibacterial and cell adhesion properties, *J. Polym. Res.* 21 (2014) 347, <https://doi.org/10.1007/s10965-013-0347-6>.
- [22] T.M. Díez-Rodríguez, et al., Nanocomposites of PCL and SBA-15 particles prepared by extrusion: structural characteristics, confinement of PCL chains within SBA-15 nanometric channels and mechanical behavior, *Polymers* 14 (2022) 129, <https://doi.org/10.3390/polym14010129>.
- [23] K. Elen, et al., Towards high-performance biopackaging: barrier and mechanical properties of dual-action polycaprolactone/zinc oxide nanocomposites, *Polym. Adv. Technol.* 23 (2012) 1422–1428, <https://doi.org/10.1002/pat.2062>.
- [24] S. Li, et al., Electrospun antibacterial poly(vinyl alcohol)/Ag nanoparticles membrane grafted with 3,3',4,4'-benzophenone tetracarboxylic acid for efficient air filtration, *Appl. Surf. Sci.* 533 (2020), 147516, <https://doi.org/10.1016/j.apsusc.2020.147516>.
- [25] F.A. Zhang, D.K. Lee, T.J. Pinnavaia, PMMA/Mesoporous silica nanocomposites: effect of framework structure and pore size on thermomechanical properties, *Polym. Chem.* 1 (2010) 107–113, <https://doi.org/10.1039/b9py00232d>.
- [26] K. Schumacher, P.I. Ravikovitch, A. du Chesne, A.V. Neimark, K.K. Unger, Characterization of MCM-48 materials, *Langmuir* 16 (2000) 4648–4654, <https://doi.org/10.1021/la991595i>.
- [27] Y. Güçbilmez, Y. Yavuz, İ. Çalıř, A. Ş Yarıç, A. S Kopal, Low temperature synthesis of MCM-48 and its adsorbent capacity for the removal of basic red 29 dye from model solutions, *Heliyon* 9 (2023), e15659, <https://doi.org/10.1016/j.heliyon.2023.e15659>.
- [28] T.W. Kim, P.W. Chung, V.S.Y. Lin, Facile synthesis of monodisperse spherical MCM-48 mesoporous silica nanoparticles with controlled particle size, *Chem. Mater.* 22 (2010) 5093–5104, https://doi.org/10.1021/cm1017344.supp_file/cm1017344_si_001.pdf.
- [29] S. Mallakpour, A. Abdolmaleki, S.E. Moosavi, Green route for the synthesis of alanine-based poly(amide-imide) nanocomposites reinforced with the modified ZnO by poly(vinyl alcohol) as a biocompatible coupling agent, *Polym. Plast. Technol. Eng.* 54 (2015) 1448–1456, <https://doi.org/10.1080/03602559.2014.996907>.
- [30] S. Mallakpour, V. Behranvand, Nanocomposites based on biosafe nano ZnO and different polymeric matrixes for antibacterial, optical, thermal and mechanical applications, *Eur. Polym. J.* 84 (2016) 377–403, <https://doi.org/10.1016/j.eurpolymj.2016.09.028>.
- [31] S. Mallakpour, S. Mansourzadeh, Sonochemical synthesis of PVA/PVP blend nanocomposite containing modified CuO nanoparticles with vitamin B1 and their antibacterial activity against *Staphylococcus aureus* and *Escherichia coli*, *Ultrason. Sonochem.* 43 (2018) 91–100, <https://doi.org/10.1016/j.ultrsonch.2017.12.052>.
- [32] H.E. Ali, et al., Microstructure study and linear/nonlinear optical performance of Bi-embedded PVP/PVA films for optoelectronic and optical cut-off applications, *Polym* 14 (2022) 1741, <https://doi.org/10.3390/polym14091741>.
- [33] S. Mallakpour, Z. Khani, Surface modified SiO₂ nanoparticles by thiamine and ultrasonication synthesis of PCL/SiO₂-VB1 NCs: morphology, thermal, mechanical and bioactivity investigations, *Ultrason. Sonochem.* 41 (2018) 527–537, <https://doi.org/10.1016/j.ultrsonch.2017.10.015>.
- [34] S. Mallakpour, N. Nouruzi, Effect of modified ZnO nanoparticles with biosafe molecule on the morphology and physicochemical properties of novel polycaprolactone nanocomposites, *Polymer (Guildf)* 89 (2016) 94–101, <https://doi.org/10.1016/j.polymer.2016.02.038>.
- [35] M. Vinícius Paula, L.A. de Azevedo, I.D.L. Silva, G.M. Vinhas, G.S. Alves Jr., Effects of gamma radiation on nanocomposite films of polycaprolactone with modified MCM-48, *Polímeros* 31 (2021), e2021031, <https://doi.org/10.1590/0104-1428.20210044>.
- [36] S. Mallakpour, N. Nouruzi, Effects of citric acid-functionalized ZnO nanoparticles on the structural, mechanical, thermal and optical properties of polycaprolactone nanocomposite films, *Mater. Chem. Phys.* 197 (2017) 129–137, <https://doi.org/10.1016/j.matchemphys.2017.05.023>.
- [37] M. Paula, I. Diego, R. Dionisio, G. Vinhas, S. Alves, Gamma irradiation effects on polycaprolactone/zinc oxide nanocomposite films, *Polímeros* 29 (2019), e2019041, <https://doi.org/10.1590/0104-1428.04018>.
- [38] R. Augustine, A. Saha, V.P. Jayachandran, S. Thomas, N. Kalarikkal, Dose-dependent effects of gamma irradiation on the materials properties and cell proliferation of electrospun polycaprolactone tissue engineering scaffolds, *Int. J. Polym. Mat. Polym. Biomater* 64 (2015) 526–533, <https://doi.org/10.1080/00914037.2014.977900>.
- [39] S. Prajapati, et al., Effect of gamma irradiation on shape memory, thermal and mechanical properties of polycaprolactone, *Radiat. Phys. Chem.* 204 (2023), 110671, <https://doi.org/10.1016/j.radphyschem.2022.110671>.
- [40] L.M. Oliveira, E.S. Araújo, S.M.L. Guedes, Gamma irradiation effects on poly(hydroxybutyrate), *Polym. Degrad. Stabil.* 91 (2006) 2157–2162, <https://doi.org/10.1016/j.polymdegradstab.2006.01.008>.
- [41] S.L. Cooke, A.R. Whittington, Influence of therapeutic radiation on polycaprolactone and polyurethane biomaterials, *Mater. Sci. Eng. C* 60 (2016) 78–83, <https://doi.org/10.1016/j.msec.2015.10.089>.
- [42] E. Cottam, D.W.L. Hukins, K. Lee, C. Hewitt, M.J. Jenkins, Effect of sterilisation by gamma irradiation on the ability of polycaprolactone (PCL) to act as a scaffold material, *Med. Eng. Phys.* 31 (2009) 221–226, <https://doi.org/10.1016/j.medengphy.2008.07.005>.
- [43] V. Masson, F. Maurin, H. Fessi, J.P. Devissaguet, Influence of sterilization processes on poly(ϵ -caprolactone) nanospheres, *Biomater* 18 (1997) 327–335, [https://doi.org/10.1016/S0142-9612\(96\)00144-5](https://doi.org/10.1016/S0142-9612(96)00144-5).
- [44] C. Pereira-Loch, R. Benavides, M.F.S. Lima, B.M. Huerta, Radiation and thermal effects on polymeric immobilization devices used in patients submitted to radiotherapy, *J. Radiother. Pract.* 11 (2012) 101–106, <https://doi.org/10.1017/S1460396911000124>.
- [45] L.A. Bosworth, A. Gibb, S. Downes, Gamma irradiation of electrospun poly(ϵ -caprolactone) fibers affects material properties but not cell response, *J. Polym. Sci. B Polym. Phys.* 50 (2012) 870–876, <https://doi.org/10.1002/polb.23072>.
- [46] L.V. Chang, H. Tian, X. Zhang, A. Xiang, LF-NMR analysis of the water mobility, state and distribution in sorbitol plasticized polyvinyl alcohol films, *Polym. Test.* 70 (2018) 67–72, <https://doi.org/10.1016/j.polymertesting.2018.06.024>.
- [47] M.F. Koenig, S.J. Huang, Biodegradable blends and composites of polycaprolactone and starch derivatives, *Polymer (Guildf)* 36 (1995) 1877–1882, [https://doi.org/10.1016/0032-3861\(95\)90934-T](https://doi.org/10.1016/0032-3861(95)90934-T).
- [48] Z. Bahrami, A. Badii, F. Atyabi, Surface functionalization of SBA-15 nanorods for anticancer drug delivery, *Chem. Eng. Res. Des.* 92 (2014) 1296–1303, <https://doi.org/10.1016/j.cherd.2013.11.007>.
- [49] S. Mallakpour, S. Rashidimoghadam, Preparation, characterization, and in vitro bioactivity study of glutaraldehyde crosslinked chitosan/poly(vinyl alcohol)/ascorbic acid-MWCNTs bionanocomposites, *Int. J. Biol. Macromol.* 144 (2020) 389–402, <https://doi.org/10.1016/j.ijbiomac.2019.12.073>.
- [50] S. Mallakpour, F. Motirasoul, Capturing Cd²⁺ ions from wastewater using PVA/ α -MnO₂-Oleic acid nanocomposites, *New J. Chem.* 42 (2018) 4297–4307, <https://doi.org/10.1039/C8NJ00304A>.
- [51] H.S. Mansur, C.M. Sadahira, A.N. Souza, A.A.P. Mansur, FTIR spectroscopy characterization of poly(vinyl alcohol) hydrogel with different hydrolysis degree and chemically crosslinked with glutaraldehyde, *Mater. Sci. Eng. C* 28 (2008) 539–548, <https://doi.org/10.1016/j.msec.2007.10.088>.
- [52] S. Subramanian, et al., Effect of gamma sterilization on *Gymnema sylvestre* leaf extract fused polycaprolactone nanofiber for effective wound dressing applications, *Mater. Lett.* 300 (2021), 130145, <https://doi.org/10.1016/j.matlet.2021.130145>.
- [53] S. Mallakpour, A. Barati, Efficient preparation of hybrid nanocomposite coatings based on poly(vinyl alcohol) and silane coupling agent modified TiO₂ nanoparticles, *Prog. Org. Coating* 71 (2011) 391–398, <https://doi.org/10.1016/j.porgcoat.2011.04.010>.

- [54] A. Abdolmaleki, S. Mallakpour, A. Karshenas, Synthesis and characterization of new nanocomposites films using alanine-Cu-functionalized graphene oxide as nanofiller and PVA as polymeric matrix for improving of their properties, *J. Solid State Chem.* 253 (2017) 398–405, <https://doi.org/10.1016/j.jssc.2017.06.014>.
- [55] S. Mallakpour, A. Abdolmaleki, Z. Khalesi, S. Borandeh, Surface functionalization of GO, preparation and characterization of PVA/TRIS-GO nanocomposites, *Polymer (Guildf)* 81 (2015) 140–150, <https://doi.org/10.1016/j.polymer.2015.11.005>.
- [56] O. Persenaire, M. Alexandre, P. Degé, P. Dubois, Mechanisms and kinetics of thermal degradation of poly(E-caprolactone), *Am. Chem. Soc.* 2 (2001) 288–294, <https://doi.org/10.1021/bm0056310>.
- [57] R.A. Ruseckaite, A. Jiménez, Thermal degradation of mixtures of polycaprolactone with cellulose derivatives, *Polym. Degrad. Stabil.* 81 (2003) 353–358, [https://doi.org/10.1016/S0141-3910\(03\)00106-X](https://doi.org/10.1016/S0141-3910(03)00106-X).
- [58] S. Mallakpour, M. Lormahdiabadi, Polycaprolactone/ZnO-Folic acid nanocomposite films: fabrication, characterization, in-vitro bioactivity, and antibacterial assessment, *Mater. Chem. Phys.* 263 (2021), 124378, <https://doi.org/10.1016/j.matchemphys.2021.124378>.
- [59] S. Mallakpour, N. Nouruzi, Modification of morphological, mechanical, optical and thermal properties in polycaprolactone-based nanocomposites by the incorporation of diacid-modified ZnO nanoparticles, *J. Math. Sci.* 51 (2016) 6400–6410, <https://doi.org/10.1007/s10853-016-9936-1>.
- [60] Y. Ji, K. Liang, X. Shen, G.L. Bowlin, Electrospinning and characterization of chitin nanofibril/polycaprolactone nanocomposite fiber mats, *Carbohydr. Polym.* 101 (2014) 68–74, <https://doi.org/10.1016/j.carbpol.2013.09.012>.
- [61] M. Bandyopadhyay, N. Tsunoji, T. Sano, Mesoporous MCM-48 immobilized with aminopropyltriethoxysilane: a potential catalyst for transesterification of triacetin, *Catal. Lett.* 147 (2017) 1040–1050, <https://doi.org/10.1007/S10562-017-1997-5/figures/11>.
- [62] M. Gil, I. Tiscornia, Ó. de la Iglesia, R. Mallada, J. Santamaría, Monoamine-grafted MCM-48: an efficient material for CO₂ removal at low partial pressures, *Chem. Eng. J.* 175 (2011) 291–297, <https://doi.org/10.1016/j.cej.2011.09.107>.
- [63] S. Kim, E. Kim, S. Kim, W. Kim, Surface modification of silica nanoparticles by UV-induced graft polymerization of methyl methacrylate, *J. Colloid Interface Sci.* 292 (2005) 93–98, <https://doi.org/10.1016/j.jcis.2005.09.046>.